

**Absorbing state phase transitions with quenched disorder**

Jef Hooyberghs

*Department WNI, Limburgs Universitair Centrum, 3590 Diepenbeek, Belgium,  
Laboratorium voor Vaste-Stoffysica en Magnetisme, Celestijnenlaan 200D, 3001 Heverlee, Belgium,  
and VITO, Flemisch Institute for Technological Research, Boeretang 200, 2400 Mol, Belgium*

Ferenc Iglói

*Research Institute for Solid State Physics and Optics, H-1525 Budapest, P. O. Box, 49, Hungary,  
and Institute of Theoretical Physics, Szeged University, H-6720 Szeged, Hungary*

Carlo Vanderzande

*Department WNI, Limburgs Universitair Centrum, 3590 Diepenbeek, Belgium  
and Instituut voor Theoretische Fysica, Celestijnenlaan 200D, 3001 Heverlee, Belgium*

(Received 3 February 2004; published 23 June 2004)

Quenched disorder—in the sense of the Harris criterion—is generally a relevant perturbation at an absorbing state phase transition point. Here using a strong disorder renormalization group framework and effective numerical methods we study the properties of random fixed points for systems in the directed percolation universality class. For strong enough disorder the critical behavior is found to be controlled by a strong disorder fixed point, which is isomorph with the fixed point of random quantum Ising systems. In this fixed point dynamical correlations are logarithmically slow and the static critical exponents are conjecturedly exact for one-dimensional systems. The renormalization group scenario is confronted with numerical results on the random contact process in one and two dimensions and satisfactory agreement is found. For weaker disorder the numerical results indicate static critical exponents which vary with the strength of disorder, whereas the dynamical correlations are compatible with two possible scenarios. Either they follow a power-law decay with a varying dynamical exponent, like in random quantum systems, or the dynamical correlations are logarithmically slow even for a weak disorder. For models in the parity conserving universality class there is no strong disorder fixed point according to our renormalization group analysis.

DOI: 10.1103/PhysRevE.69.066140

PACS number(s): 05.70.Ln, 05.70.Jk, 64.60.Ak

**I. INTRODUCTION**

Nonequilibrium many-particle systems are often described by stochastic models in which some degrees of freedom with fast relaxation behavior are integrated out and are replaced by a noise term, which may represent thermal or quantum fluctuations, chaotic motion, etc. The classification of steady states of these nonequilibrium models is an important task and we are currently witnessing considerable theoretical progress in this field. Of particular interest are systems that in the steady state show long-range spatial and temporal correlations, as is the case when they are in the vicinity of a nonequilibrium phase transition point. A special type of these are the transitions between an active phase and an inactive one where the particles are absorbed into a state without fluctuations. These absorbing state phase transitions play an important role in physics, chemistry, and even biology [1,2].

Classification of absorbing state phase transitions has shown that the universality class of directed percolation is particularly robust. It contains models with a scalar order parameter, absence of conservation laws, and short range interactions [3]. Well known models with a phase transition in this universality class are the contact process [4] and the Ziff-Gulari-Barshad model of catalytic reactions [5]. When there is a conservation law present, other universality classes can appear, the best known of which is the parity conserving class [6] which includes the branching–annihilating random

walk with even number of offspring [6,7] and the generalized contact process with two different absorbing states [8]. Most recently reaction-diffusion models with multiple branching and annihilation processes were also intensively studied [9]. Sandpile models with conserved energy can also be related to absorbing state phase transitions [10].

Quenched, i.e. time-independent, disorder is an inevitable feature of many real processes and could play an important role in stochastic particle systems too. As an example, it has been argued that due to the presence of some form of disorder the directed percolation universality class has not yet been seen in real experiments [11], such as in catalytic reactions [5], in depinning transitions [12], and in the flow of granular matter [13] (for a review, see [11]). In stochastic particle systems, disorder is represented by position dependent reaction rates and its relevance can be expressed in a  $(d+1)$ -dimensional system by a Harris-type criterion [14],

$$\nu_{\perp} < 2/d. \quad (1)$$

Here  $\nu_{\perp}$  is the correlation length exponent in the spatial direction of the pure system. Indeed for directed percolation at any  $d < 4$  dimensions the disorder is a relevant perturbation.

The new, random fixed points, which control the critical behavior of absorbing state systems with quenched disorder have been studied in different papers and their properties are

found in some respect to be unconventional [14–19]. Early numerical studies by Noest [14] on random cellular automaton models in the directed percolation universality class in one and two dimensions have shown considerable change of the critical exponents in comparison with the pure system’s values. In more recent studies [15] of the two-dimensional contact process with dilution, logarithmically slow dynamical correlations were found. These could be related to the results of a field-theoretical investigation by Janssen [16], according to which the renormalization group equations have only runaway solutions. Interestingly the exponents, associated with the logarithmic time-dependence of different dynamical quantities were found to be disorder dependent. The absorbing phase was found to have properties similar to that of a Griffiths phase and shows power law behavior with non-universal exponents [15,17,18]. The static critical behavior of the model has been explored less, but exponents in  $d=2$  have been determined [15].

In the present paper we revisit the problem of absorbing state phase transitions in the presence of quenched disorder. In this study we make use of the formal analogy between quantum systems and the “Hamiltonian” operator formalism [20,21] of stochastic processes. Although the latter operators are generally non-Hermitian, techniques developed in the study of quantum spin systems can often be successfully applied [21–24].

In the theory of random quantum spin systems, recently considerable progress has been made in understanding their low-energy (or long time), long distance behavior. In particular, the use of a real space renormalization group (RG) method, originally introduced by Ma, Dasgupta, and Hu [25] has led to many new, partially exact results and has given—at the same time—new physical insight into the problem [26]. Subsequent analytical and numerical work has provided further important results, in particular for one-dimensional systems [26–28]. One new concept which has emerged from these studies is the existence of strong disorder fixed points in which the disorder plays a completely dominant role. This property is manifested by the fact that during renormalization, the distribution of the random parameters (couplings, transverse fields, etc.) broaden without limits and therefore the RG treatment becomes asymptotically exact.

Having the close similarity between quantum systems and the Hamiltonian description of stochastic processes, one might ask the question if the concept of strong disorder fixed point applies for the latter in the presence of quenched disorder. For what is perhaps the simplest stochastic process, the random walk, the answer is positive. Sinai diffusion [29], which represents a particular type of random walk in a random environment, can be interpreted as a realization of a strong disorder fixed point. Indeed RG methods have been successfully applied to explore new exact properties of this process [30].

While the Sinai diffusion obeys detailed balance, most of the stochastic particle systems do not. Therefore it is particularly interesting to know if quenched disorder could have a similar effect on the latter problems, too. In this paper we are going to study this issue in detail. In particular we investigate the applicability of the strong disorder RG scheme for mod-

els in different (nonrandom) universality classes. The RG predictions are then confronted with the results of extensive numerical calculations, which are performed by density matrix renormalization (DMRG) and by Monte Carlo (MC) simulations. A short account of our results has been published in a Letter [31].

The structure of the paper is the following. General notations about scaling theory at absorbing state phase transitions, both at conventional and strong disorder fixed points, are given in Sec. II. The method of strong disorder renormalization group is explained in detail in Sec. III, where it is applied to the random contact process and to its generalization with two different absorbing states. Results on random directed percolation are obtained by mapping onto a random walk. Sec. IV contains a comparison of these analytical predictions with results of numerical calculations on the one- and two-dimensional contact process. Our conclusions are presented in the final section, and some technical details are given in the Appendixes.

## II. SCALING AT ABSORBING STATE PHASE TRANSITIONS

In the models that we consider here each site,  $i$ , of a  $d$ -dimensional lattice is either vacant ( $\emptyset$ ) or occupied by at most one particle ( $A$ ). The dynamics of the model is given by a continuous time Markov process and is therefore defined in terms of transition rates. The reactions in the system are basically of two types: (a) branching in which particles are created at empty sites (provided one of its neighbors is occupied) occurs with rate  $\lambda_i$ , and death of particles with a rate,  $\mu_i$ . The average number of particles at site  $i$ , at a given time  $t$  is denoted by  $\langle n_i \rangle(t)$ . This system evolves to a stationary state in which averages become time independent. In this state, if the average value of the branching rates compared with the average value of the death rates is sufficiently large, a finite fraction of sites,  $\rho = L^{-1} \sum_i \langle n_i \rangle > 0$ , is occupied and the system is in the active phase. In the opposite situation, i.e. when the average value of the branching rates is relatively small, then  $\rho=0$  and the system is in the inactive phase. The two phases described above are separated by a phase transition point, which is located at  $\Delta = \Delta_c$ , where  $\Delta$  is a suitably defined control parameter. In the homogeneous system with  $\mu_i = \mu$  and  $\lambda_i = \lambda$  we have  $\Delta = \mu/\lambda$ .

### A. Conventional scaling behavior

In the vicinity of the nonequilibrium phase-transition point, where the reduced control parameter  $\delta = (\Delta - \Delta_c)/\Delta_c$  is small, generally anisotropic space-time scaling symmetry holds. The order-parameter,  $\rho(\delta, 1/t, 1/L)$ , as a function of a finite time-scale  $t$ , in a large finite system of size  $L$ , scales under changing lengths by a factor  $b > 1$ ,  $L' = L/b$ , as [2,3]

$$\rho(\delta, 1/t, 1/L) = b^{-x} \rho(\delta b^{1/\nu_\perp}, b^z/t, b/L). \quad (2)$$

Here the critical exponents,  $x$ ,  $\nu_\perp$  and  $z$  have the usual definitions: the correlation length  $\xi_\perp$  in the spatial (the relaxation time  $t_r$  or the correlation length  $\xi_\parallel$  in the temporal) direction diverges as  $\xi_\perp \sim |\delta|^{-\nu_\perp}$  ( $t_r = \xi_\parallel \sim |\delta|^{-\nu_\parallel}$ ) and the anisotropy or

dynamical exponent is defined as  $z = \nu_{\parallel} / \nu_{\perp}$ . Taking the scaling parameter  $b = \delta^{-\nu_{\perp}}$  we have in the thermodynamic limit,  $1/L=0$  and in the stationary state ( $1/t=0$ ),  $\rho(\delta) \sim \delta^{\beta}$  with the order-parameter exponent  $\beta = x\nu_{\perp}$ . For a surface site one defines the surface order-parameter,  $\rho_s$ , the scaling behavior of which is the same as in Eq. (2) but involves the surface scaling dimension,  $x_s$ , instead of the bulk exponent  $x$  so that  $\rho_s(\delta) \sim \delta^{\beta_s}$  with  $\beta_s = x_s\nu_{\perp}$  [32].

The dynamical behavior of stochastic systems is related to the scaling properties of the characteristic time,  $t_r$ , which in the Hamiltonian formalism is given by the inverse of the smallest gap,  $\epsilon$ . In a conventional fixed point we have the relation

$$\epsilon(\delta, 1/t, 1/L) = b^{-z} \epsilon(\delta b^{1/\nu_{\perp}}, b^z/t, b/L); \quad (3)$$

thus in a finite system the appropriate scaling combination is  $\epsilon L^z$ .

The autocorrelation function,  $G(\delta, 1/t, 1/L) = \langle n_i(t)n_i(0) \rangle$ , which, at least for a homogeneous system, is independent of the position of a particle in the bulk, has the scaling behavior at the transition point:

$$G(\delta = 0, 1/t, 1/L) = b^{-2x} G(\delta = 0, b^z/t, b/L). \quad (4)$$

Here, taking  $b = t^{1/z}$  we obtain in the thermodynamic limit  $G(t) \sim t^{-2x/z}$ .

In a MC simulation one usually starts with one seed-particle in the origin of an empty lattice and measures the survival probability at the origin,  $P_s$ , the total number of particles present in the system,  $N$ , and the mean-square distance of the particles from the origin,  $R^2$ . For the contact process it can be shown [3,33] that in the long time limit, the survival probability equals the local order parameter. This ‘‘duality’’ relation also holds in the disordered case. More generally, it is expected that if there is only one absorbing state, the two quantities are expected to obey the same scaling behavior [2]. Thus from Eq. (2) we then immediately get

$$P_s(\delta, 1/t, 1/L) = b^{-x} P_s(\delta b^{1/\nu_{\perp}}, b^z/t, b/L). \quad (5)$$

For  $b = t^{1/z}$  we obtain at the critical point,  $P_s(t) \sim t^{-\theta}$  with  $\theta = x/z = \beta/(\nu_{\perp}z)$ . Generally we have  $G(t) \sim P_s^2(t)$ . The total number of particles is proportional to the integral of the density–density correlation function and obeys the scaling relation

$$N(\delta, 1/t, 1/L) = b^{d-2x} N(\delta b^{1/\nu_{\perp}}, b^z/t, b/L). \quad (6)$$

It therefore behaves at the critical point as  $N(t) \sim t^{\eta}$ , with  $\eta = (d-2x)/z$ . Finally,  $R^2$  scales similarly as  $L^2$ :

$$R^2(\delta, 1/t, 1/L) = b^2 R^2(\delta b^{1/\nu_{\perp}}, b^z/t, b/L), \quad (7)$$

and at the critical point we have  $R^2(t) \sim t^{2/z}$ . We note that in the general situation, i.e., when several absorbing states exist, the scaling relations in Eqs. (5)–(7) involve a new exponent,  $x'$ , instead of  $x$ .

For further comparisons, we quote the current estimates of the various critical exponents for the case of the homogeneous, one-dimensional contact process [2,32]:  $x=0.2524$ ,  $\nu_{\perp}=1.0972$ ,  $z=1.582$  and  $x_s=0.669$ .

## B. Strong disorder scaling

Strong disorder fixed points were observed so far in random quantum systems as well as in Sinai diffusion. Here we suggest that the same type of fixed point can also exist in absorbing state phase transitions and we introduce the corresponding scaling theory, which is based on two ingredients [34]. First, at a strong disorder fixed point the dynamical behavior is ultraslow. The characteristic length-scale,  $\xi$ , is related to the logarithm of the characteristic time-scale,  $t_r$ , as

$$\xi^{\psi} \sim \ln t_r; \quad (8)$$

thus the dynamical exponent,  $z$ , is formally infinity. Second, the average value of quantities related to the particle occupation number are dominated by so called *rare events* (or rare regions of a large sample). In a rare event  $\langle n_i \rangle = O(1)$ , thus  $L$  independent, whereas in a *typical realization*  $\langle n_i \rangle$ , is generally exponentially small in  $L$ . The fraction of rare events,  $f$ , is decreasing with the size,  $L$ . At the critical point we can write for it the scaling transformation:

$$f(1/L) = b^{-x} f(b/L); \quad (9)$$

thus with  $b=L$  we have  $f \sim L^{-x}$ . The average value of the particle density is indeed dominated by the rare events; thus  $\rho \sim f$ , and the order-parameter at the critical point satisfies the scaling transformation:

$$\rho(\delta, 1/\ln t, 1/L) = b^{-x} \rho(\delta b^{1/\nu_{\perp}}, b^{\psi}/\ln t, b/L). \quad (10)$$

One can see that the static exponents,  $\beta = x\nu_{\perp}$  and  $\beta_s = x_s\nu_{\perp}$ , are given by the same expressions as in the case of ordinary scaling. (We shall explicitly show the construction of rare events for random directed percolation in Sec. III B 2.)

Due to the ultraslow dynamical behavior the scaling relation (3) is modified into

$$\ln \epsilon(\delta, 1/\ln t, 1/L) = b^{-\psi} \ln \epsilon(\delta b^{1/\nu_{\perp}}, b^{\psi}/\ln t, b/L); \quad (11)$$

thus in a finite system the appropriate scaling combination is  $(\ln \epsilon) L^{\psi}$ .

To calculate the average autocorrelation function one should keep in mind that disorder in the time-direction is strictly correlated; thus in a rare event the autocorrelation function is of  $O(1)$  and (almost) zero otherwise. Thus the average autocorrelation function is proportional to the fraction of rare events,  $G \sim f$ , and scales at the critical point:

$$G(\delta = 0, 1/\ln t, 1/L) = b^{-x} G(\delta = 0, b^{\psi}/\ln t, b/L). \quad (12)$$

Thus in the thermodynamic limit,  $G(t) \sim (\ln t)^{-x/\psi}$ . We can also determine the scaling behavior of other dynamical quantities such as  $P_s$ ,  $N$ , and  $R^2$ , in the strong disorder fixed point in a similar way. It is therefore sufficient to replace in the conventional scaling relations in Eqs. (5)–(7)  $t$  by  $\ln t$  and  $z$  by  $\psi$ . As a consequence the time-dependence of the dynamical quantities will also be logarithmic at the critical point:

$$P_s(t) \sim (\ln t)^{-\bar{\theta}}, \quad \bar{\theta} = x/\psi,$$

$$\begin{aligned}
 N(t) &\sim (\ln t)^{\bar{\eta}}, \quad \bar{\eta} = (d - 2x)/\psi, \\
 R^2(t) &\sim (\ln t)^{\bar{\sigma}}, \quad \bar{\sigma} = 2/\psi.
 \end{aligned}
 \tag{13}$$

This type of logarithmic time dependence has been observed by Dickman and Moreira [15] by analyzing numerical data on the diluted 2d contact process, and were interpreted as a “violation of scaling.” The measured exponents  $\bar{\theta}$ ,  $\bar{\eta}$ , and  $\bar{\sigma}$  were found to be dilution, i.e. disorder, dependent.

In the following, using a real space renormalization group method we (i) shall give a natural explanation of the observed logarithmic time dependence and (ii) shall calculate the critical exponents, which—in the one-dimensional case—are presumably exact.

### C. Scaling in the Griffiths-phase

In a disordered nonequilibrium system, which is globally in one stationary phase, say in the nonactive phase with  $\delta > 0$ , there are specific local regions of size  $l_c$ , in which strong fluctuations of the local rates prefer the existence of the other phase, say the active phase. These rare regions, which are localized and have an exponentially small probability of occurrence,  $p(l_c) \sim \exp(-\alpha l_c)$ , contribute to an exponentially large relaxation time [35],  $t_r \sim \exp(\sigma l_c)$ . (In a  $d$ -dimensional system  $l_c$  should be replaced by  $l_c^d$ .) Then the distribution of large relaxation times has an algebraic tail:  $p(t_r) \sim t_r^{-1/z'-1}$ , with  $1/z' = \beta/\sigma$  and the average autocorrelation function:

$$G(t) \sim \int dt_r p(t_r) \exp(-t/t_r) \sim t^{-1/z'}
 \tag{14}$$

also decays algebraically. Consequently in this so called Griffiths phase [36] dynamical correlations are quasi-long-ranged, whereas spatial correlations are short ranged. The dynamical exponent is a continuously varying function of the distance from the critical point,  $z' = z'(\delta)$ .

This result can be incorporated into a scaling theory as follows. Since a rare event, which brings the dominant contribution to the average autocorrelation function is localized, its probability of occurrence is inversely proportional with the size of the system,  $L$ . Consequently the average autocorrelation function obeys the scaling law

$$G(\delta, 1/t, 1/L) = b^{-1} G(\delta, b^{z'}/t, b/L),
 \tag{15}$$

and with  $b = t^{1/z'}$  we recover in the thermodynamic limit the relation in Eq. (14). Finally, scaling of the lowest gaps follow the rule

$$\epsilon(\delta, 1/t, 1/L) = b^{-z'} \epsilon(\delta, b^{z'}/t, b/L);
 \tag{16}$$

thus in a finite system the appropriate scaling combination is  $\epsilon L^{z'}$ . We note that in the Griffiths phase the power-law singularities are often supplemented by logarithmic corrections [38,39], which are related to the fact that the size of the rare event grows logarithmically,  $l_c \sim \ln L$ , since  $p(l_c) \sim 1/L$ .

## III. THE RENORMALIZATION GROUP FRAMEWORK

In this section we apply a real space renormalization group method for random stochastic particle systems, which is a variant of the Ma-Dasgupta-Hu method originally developed to study random quantum spin chains [25]. The essence of the method can be summarized in the following points.

(i) Start with the initial distribution of the random reaction rates,  $P_{\text{in}}(\mu)$  and  $R_{\text{in}}(\lambda)$  and sort the rates in descending order. The largest rate, i.e. the fastest process, sets the energy scale,  $\Omega$ , in the problem.

(ii) Integrate out the fastest local process, i.e. eliminate the rate,  $\Omega$ . This amounts to decimate out one site of the lattice or to replace a pair of sites with a new effective one. Renormalized couplings are then determined using a second order perturbation calculation. It is interesting to remark that for stochastic systems this step corresponds to a fast rate expansion as discussed in Sec. 4.3 of Ref. [21].

(iii) Iterate the decimation process. This will result in a reduction of the energy-scale,  $\Omega$ , and a modification of the distribution of the (effective) rates:  $P(\mu, \Omega)$  and  $R(\lambda, \Omega)$ .

(iv) At the fixed point of the transformation (which is at  $\Omega = \Omega^* = 0$ ) the distributions of the rates become singular and from these singularities the value of the critical exponents are calculated.

In the following we construct and solve the RG equations explicitly for the random contact process.

### A. The random contact process

#### 1. The Hamiltonian formalism

In the contact process each site of the lattice can be either vacant ( $\emptyset$ ) or occupied by at most one particle ( $A$ ), and thus can be characterized by an Ising-spin variable,  $\sigma_i = 1$  for  $\emptyset$  and  $\sigma_i = -1$  for  $A$ . The state of the system is then given by the vector  $\mathbf{P}(\sigma, t)$  which gives the probability that the system is in the state  $\sigma = \{\dots, \sigma_i, \dots\}$  at time  $t$ . A particle can be created at an empty site  $i$  with a rate  $p \hat{\lambda}_i / p_0$ , where  $p(p_0)$  is the number of occupied neighbors (the coordination number of the lattice) and at an occupied site the particle is annihilated with a rate  $\mu_i$ . The time evolution is governed by a master equation, which can be written in the form

$$\frac{d\mathbf{P}(\sigma)}{dt} = -H_{CP}\mathbf{P}(\sigma).
 \tag{17}$$

Here the generator  $H_{CP}$  of the Markov process is given by:

$$H_{CP} = \sum_i \mu_i M_i + \sum_{\langle ij \rangle} \frac{\hat{\lambda}_i}{p_0} (n_i Q_j + Q_i n_j),
 \tag{18}$$

in terms of the matrices

$$M = \begin{pmatrix} 0 & -1 \\ 0 & 1 \end{pmatrix}, \quad n = \begin{pmatrix} 0 & 0 \\ 0 & 1 \end{pmatrix}, \quad Q = \begin{pmatrix} 1 & 0 \\ -1 & 0 \end{pmatrix},$$

and  $\langle ij \rangle$  stands for nearest neighbors. It is well known [21] that the steady state probability distribution of a stochastic process coincides with the ground state of its generator (sometimes also called quantum Hamiltonian of the stochas-



tic process) while relaxation properties can be determined from its low lying spectrum.

For nonrandom couplings there is a nonequilibrium phase transition in the contact process which belongs to the universality class of directed percolation [2,3]. In one dimension it is at  $(\mu/\hat{\lambda})_c=0.3032$  and the critical exponents are given by  $\beta=0.2765$ ,  $\beta_s=0.7337$ ,  $\nu_{\perp}=1.097$  and  $z=1.581$ . In two dimensions  $(\mu/\hat{\lambda})_c=0.6065$  and  $\beta=0.584$ ,  $\beta_s=1.03$ ,  $\nu_{\perp}=0.734$  and  $z=1.76$ . In the following we often use the variable  $\lambda=\hat{\lambda}/p_0$  to characterize the creation rate.

## 2. Decimation rules of the random process

For the random contact process the transition rates  $\mu_i$  and  $\lambda_i$  are independent and identically distributed variables and, as described in the previous section, the largest one  $\Omega=\max(\{\lambda_i\},\{\mu_i\})$  sets the energy scale in the system. Thus, the largest rate can be either one of the death rates  $\mu_i$  or be one of the branching rates  $\lambda_i$ . For each a different way of decimation should be used.

(i) *The largest term is a branching rate:*  $\Omega=\lambda_2$ . If the largest rate is a branching, say  $\lambda_2$ , which connects sites  $i=2$  and  $j=3$ , the two-site cluster (2,3) spends most of the time in the configurations  $AA$  or  $\emptyset\emptyset$  and can be rarely found in one of the other two configurations,  $A\emptyset$  and  $\emptyset A$ . Consequently for large times the two sites behave as a cluster with a moment of  $\tilde{m}=2$  and with an effective death rate,  $\tilde{\mu}_2$ , which can be calculated from the energy spectrum of the two-site Hamiltonian,  $H_{CP}^{23}$ . As shown in Appendix A the two lowest energy levels of the cluster are separated from the two others by a distance of  $\lambda_2$ , therefore in a good approximation just the two lowest levels can be retained. The effective death rate,  $\tilde{\mu}$ , is given from the value of the lowest gap as

$$\tilde{\mu} = \frac{2\mu_2\mu_3}{\lambda_2}, \quad (19)$$

where  $\mu_2$  and  $\mu_3$  are the original death rates at sites  $i=2$  and  $j=3$ , respectively. The renormalization equation in Eq. (19) should be extended by the renormalization of moments (i.e., the number of original sites in the cluster):

$$\tilde{m} = m_2 + m_3, \quad (20)$$

where in the initial situation  $m_2=m_3=1$ .

The renormalized value of the death rate can also be obtained with the following reasoning. Let us start with the original representation, when the two-site cluster is in the occupied state,  $AA$ . In the effective decay process first the particle at site 2 should decay (with rate  $\mu_2$ ), which is then followed by the decay of the particle at 3. This second process has a very low probability of  $\mu_3/(\lambda_2+\mu_3)$ . Since the same processes can also occur with the role of 2 and 3 interchanged, we find that for  $\lambda_2 \gg \mu_2, \mu_3$  the effective decay rate is given in Eq. (19).

(ii) *The largest term is a death rate:*  $\Omega=\mu_2$ . In this case the site (2) is almost always empty,  $\emptyset$ , therefore it does not contribute to the fractal properties of the  $A$  cluster and can be decimated out. The effective branching rate,  $\tilde{\lambda}$  between the

remaining sites 1 and 3 can be obtained by studying the eigenvalues of the three-site Hamiltonian,  $H_{CP}^{123}$ . As shown in the Appendix A out of the eight eigenvalues there are four of  $O(\mu_2)$ , which are discarded. The remaining lowest four levels are identified as the spectrum of a two-site cluster with an effective branching rate:

$$\tilde{\lambda} = \frac{\lambda_2\lambda_3}{\mu_2}. \quad (21)$$

As in the previous case one can obtain the renormalized value of the branching rate with a simple reasoning, which works as follows. Let us have the configuration of the three-site cluster in the original representation as  $A\emptyset\emptyset$ . The effective branching rate between sites 1 and 3 is generated by a virtual process, in which first a particle is created at site 2 (rate  $\lambda_2$ ), and then one at site 3 [probability  $\lambda_3/(\lambda_3+\mu_2)$ ]. Hence, we get for very strong disorder the branching rate given in Eq. (21).

The renormalization equations in Eqs. (19) and (21) can be transformed into a symmetric form in terms of the variable,  $J=\lambda/\kappa=\hat{\lambda}/(p_0\kappa)$  with  $\kappa=\sqrt{2}$  as

$$\tilde{\mu} = \kappa \frac{\mu\mu'}{J}, \quad \tilde{m} = m + m', \quad \tilde{J} = \kappa \frac{JJ'}{\mu}. \quad (22)$$

We can see from Eq. (22) that for a weak disorder the generated new rates can be occasionally larger than the decimated ones; thus in these steps the energy-scale does not lower. For a strong enough disorder, however, these non-monotonic steps are expected to be so rare that they do not influence the behavior of the RG flow. With this assumption we analyze in the following the properties of the RG equations in one dimension. The results are then confronted with numerical calculations in Sec. IV.

## 3. Renormalization in one dimension

In one dimension the topology of the lattice does not change under renormalization which makes it possible to treat the problem analytically. First we note that after repeated use of the transformations in Eq. (22) the generated branching (death) rates are in the form of a ratio of products of original branching (death) rates and original death (branching) rates. The control parameter,  $\delta$ , is defined as

$$\delta = \frac{[\ln \mu]_{\text{av}} - [\ln J]_{\text{av}}}{\text{var}[\ln \mu] + \text{var}[\ln J]}, \quad (23)$$

and at the fixed point,  $\delta=0$ , which follows from duality of the RG equations in Eq. (22) (here  $[\cdot]_{\text{av}}$  denotes the average over the disorder).

At a given energy scale,  $\Omega$ , we have the distribution function of the death rates,  $P(\mu, \Omega)$ , and that of the branching rates,  $R(J, \Omega)$ . Changing the energy scale,  $\Omega \rightarrow \Omega - d\Omega$ , amounts to eliminate a fraction of  $d\Omega[P(\Omega, \Omega) + R(\Omega, \Omega)]$  sites. The distribution of the branching rates changes as:

$$\begin{aligned}
 R(J, \Omega - d\Omega) = & \left\{ R(J, \Omega) \right. \\
 & + d\Omega P(\Omega, \Omega) \int_0^\Omega dJ_1 \int_0^\Omega dJ_3 R(J_1, \Omega) R(J_3, \Omega) \\
 & \times \left[ \delta\left(J - \frac{\kappa J_1 J_3}{\Omega}\right) - \delta(J - J_1) - \delta(J - J_3) \right] \left. \right\} \\
 & \times \{1 - d\Omega [P(\Omega, \Omega) + R(\Omega, \Omega)]\}^{-1}. \quad (24)
 \end{aligned}$$

Here on the r.h.s. the three delta functions represent the one generated new branching rate and the two decimated branching rates during one RG step and the second factor ensures normalization. [37]. A similar equation is obtained for the distribution of the death rates. From the duality of the RG equations, it follows that one should only make the interchange  $\mu \leftrightarrow J$  and  $P \leftrightarrow R$ .

Expanding  $R(J, \Omega - d\Omega)$  one arrives at the integro-differential equation:

$$\begin{aligned}
 \frac{dR}{d\Omega} = & R(J, \Omega) [P(\Omega, \Omega) - R(\Omega, \Omega)] \\
 & - P(\Omega, \Omega) \int_{J/\kappa}^\Omega dJ' R(J', \Omega) R\left(\frac{J}{J'\kappa}, \Omega\right) \frac{\Omega}{J'\kappa}, \quad (25)
 \end{aligned}$$

and similarly one obtains for the distribution  $P(\mu, \Omega)$ ,

$$\begin{aligned}
 \frac{dP}{d\Omega} = & P(\mu, \Omega) [R(\Omega, \Omega) - P(\Omega, \Omega)] \\
 & - R(\Omega, \Omega) \int_{\mu/\kappa}^\Omega d\mu' P(\mu', \Omega) P\left(\frac{\mu}{\mu'\kappa}, \Omega\right) \frac{\Omega}{\mu'\kappa}. \quad (26)
 \end{aligned}$$

A solution of these equations can be obtained analytically at the fixed point,  $\Omega=0$ , at  $\delta=0$ , in which the distributions  $R(J, \Omega)$  and  $P(\mu, \Omega)$  are asymptotically identical. The calculations can be found in Appendix B. According to these results the appropriate scaling variable is in logarithmic form  $\eta = -(\ln \Omega - \ln J) / \ln \Omega = -(\ln \Omega - \ln \mu) / \ln \Omega$ , and its distribution is given from Eqs. (B1) and (B8) as

$$p(\eta) d\eta = \exp(-\eta) d\eta. \quad (27)$$

The distribution in terms of the original variables,  $J$  (and  $\mu$ ) in Eq. (B2), is given by

$$R(J, \Omega) = \tilde{R} \left( \frac{\Omega}{J} \right)^{1-\tilde{R}\Omega}, \quad \tilde{R}\Omega = \frac{1}{\ln(\Omega_0/\Omega)}, \quad (28)$$

where  $\Omega_0$  is a reference energy scale, and the distribution becomes singular at the fixed point, as  $\Omega \rightarrow 0$ . Due to this singularity the decimation transformation in Eq. (22) becomes exact at the fixed point. This can be shown by calculating the probability that one of the neighboring death rates, besides the largest branching rate with  $J=\Omega$ , has a value of  $\mu > \alpha\Omega$ , with  $\alpha < 1$ :

$$P(\alpha) \approx \int_{\alpha\Omega}^\Omega P(J, \Omega) dJ = \tilde{R}\Omega \int_{\alpha}^1 x^{-1+\tilde{R}\Omega} dx \approx \tilde{R}\Omega \ln(1/\alpha), \quad (29)$$

which indeed goes to zero as the iteration proceeds, since  $\tilde{R}\Omega \rightarrow 0$ . Consequently the RG transformation becomes asymptotically exact and the singularities, calculated by this method at the critical point, are also very probably exact.

We start to determine the relation between the energy scale,  $\Omega$ , and the length scale,  $L_\Omega$ , by studying the fraction of nondecimated sites,  $n_\Omega$ . When the energy scale is decreased by an amount of  $d\Omega$  a fraction of sites,  $dn_\Omega = n_\Omega [\tilde{P}(\Omega) + \tilde{R}(\Omega)]$ , is decimated out, so that we obtain the differential equation:

$$\frac{dn_\Omega}{d\Omega} = n_\Omega [\tilde{P}(\Omega) + \tilde{R}(\Omega)], \quad (30)$$

which can be rewritten as

$$-\frac{d \ln n_\Omega}{d \ln \Omega} = -\Omega [\tilde{P}(\Omega) + \tilde{R}(\Omega)] = -2y(\Omega). \quad (31)$$

Using the solution to  $y(\Omega)$  in Eq. (B8) one can integrate Eq. (31) with the result

$$n_\Omega = \left[ 1 + y_0 \ln \frac{\Omega_0}{\Omega} \right]^{-2} \sim \left[ \ln \frac{\Omega_0}{\Omega} \right]^{-2}, \quad \delta = 0. \quad (32)$$

Thus from Eq. (32) we get for the typical distance between remaining spins,  $L_\Omega$ , as

$$L_\Omega \sim \frac{1}{n_\Omega} \sim \left[ \ln \frac{\Omega_0}{\Omega} \right]^2, \quad \delta = 0. \quad (33)$$

This is equivalent with a logarithmic dynamical scaling as written in Eq. (8) with an exponent,  $\psi = 1/2$ .

In order to calculate the singularity of other quantities, such as the correlation length and the order-parameter, at the fixed point we should study scaling of the lengths and the cluster moments. As we have shown in the Appendix C, at the fixed point these calculations are equivalent to that for the random transverse Ising spin chain. Therefore here we quote only the results. For a detailed derivation we refer to the original literature [26,39].

We are reminded first that a renormalized site is composed from parts of the original lattice and the renormalized length is given by the sum of the lengths in the original lattice. In the paramagnetic phase the average length of sites approach a finite value,  $\xi_\perp$ , during renormalization as  $\Omega \rightarrow 0$ . In the vicinity of the fixed point the RG-equations lead to a singularity:

$$\xi_\perp \sim |\delta|^{-\nu_\perp}, \quad \nu_\perp = 2. \quad (34)$$

To study scaling of the order-parameter one should investigate the average cluster moment, which at the critical point behaves as

$$\bar{m} = \bar{m}_0 \left[ \ln \left( \frac{\Omega_0}{\Omega} \right) \right]^\Phi, \quad \Phi = \frac{1}{\tau} = \frac{1 + \sqrt{5}}{2}. \quad (35)$$

Then the order-parameter can be calculated as  $\rho = \bar{m}/L_\Omega$ , which behaves asymptotically as

$$\rho \sim L^{-x}, \quad (36)$$

and the scaling dimension,  $x$ , is given by Eqs. (33) and (35) as

$$x = \frac{2 - \Phi}{2}. \quad (37)$$

Finally, scaling of the surface order-parameter is related to the average cluster moment of the surface site,  $\bar{m}_s$ . This is naturally smaller than for a bulk site, since the surface moment can accumulate from original sites only in one direction. According to an analysis of the RG results we have

$$\bar{m}_s = \bar{m}_{s0} \left[ \ln \left( \frac{\Omega_0}{\Omega} \right) \right]; \quad (38)$$

thus

$$\rho_s \sim L^{-x_s}, \quad x_s = 1/2. \quad (39)$$

#### 4. Renormalization in two dimensions

In higher dimensions the topology of the lattice changes under renormalization: contacts and therefore reactions are generated between remote sites, too. However, the renormalization does not introduce new types of reactions. Therefore the renormalization process, which is summarized in the decimation equations in Eq. (22) can be implemented numerically. As in one dimension for a weak disorder the generated new couplings are frequently larger than the decimated ones; therefore the RG scheme does not work and scaling in the random system is most probably conventional, as described in Sec. II A. For a stronger disorder, however, the situation could change and strong disorder scaling could set in. If the critical behavior of the system is indeed attracted by a strong disorder fixed point, then, as in one dimension, the value of a finite pre-factor  $\kappa > 0$  in Eq. (22) does not matter. Numerical renormalization group calculations for the random transverse-field Ising model, for which  $\kappa = 1$ , have shown the existence of a strong disorder fixed point in two-dimensions [40,41]. The numerically observed critical exponents are  $x = 1.0$ ,  $\nu_\perp = 1.07$  and  $\psi = 0.42$  [40]. Karevski *et al.* [41] use a somewhat different numerical technique and find  $x = 0.97$ ,  $\nu_\perp = 1.25$  and  $\psi = 0.5$ . In light of the above arguments we expect also for the two-dimensional random contact process strong disorder scaling with the above exponents in Eq. (10) if the strength of disorder is sufficiently large. To verify this scenario we shall reanalyze the numerical results of Moreira and Dickman [15] in Sec IV B.

#### B. Random directed percolation

Directed percolation can be viewed as an anisotropic variant of percolation, in which the possible path of occupied

sites follows a given preferential direction. Equivalently, directed percolation can be interpreted as a dynamical process, in which the spreading of a nonconserved agent is studied. In the random version of the problem the occupation probabilities are random variables, which are strictly correlated along the preferential (time) direction, corresponding to random reaction rates in the dynamical interpretation.

#### 1. Random Reggeon field theory

The field theory, which is expected to describe the critical behavior of directed percolation is the Reggeon field theory. In (1+1)-dimension in the Hamiltonian limit the time-evolution of the process is governed by the Hamiltonian [42]  $H_{RF} = \sum_i H_i$  with

$$H_i = -h_i \sigma_i^x - \frac{g_i}{2} [(1 - 2\sigma_i^+) (1 - 2\sigma_{i+1}^+) - \sigma_i^z \sigma_{i+1}^z], \quad (40)$$

where  $\sigma_i^{x,y,z}$  are Pauli matrices at site  $i$ , and  $\sigma_i^\pm = (\sigma_i^x \pm i\sigma_i^y)/2$ . The structure of  $H_{RF}$  is similar to the Hamiltonian of the random transverse-field Ising model in Eq. (18): it consists of an interaction term (which is non-Hermitian in  $H_{RF}$ ) and a transverse field term. The order in the system is measured by the asymptotic limit of the autocorrelation function,  $G(t) = \langle 0 | \sigma_i^z(t) \sigma_i^z(0) | 0 \rangle_{\text{av}}$ : it is zero in the paramagnetic phase and finite in the ordered phase.

The renormalization of the random Reggeon-field theory can be made in a way that is completely similar to that for the random contact process (or the random transverse-field Ising model). A very strong coupling,  $g_2 = \Omega$ , will result in a two-site cluster in a renormalized field which is given by

$$\tilde{h} = \frac{2h_2 h_3}{g_2}. \quad (41)$$

On the other hand a site on which a very strong field,  $h_2 = \Omega$ , acts is decimated out and a new coupling is generated between remaining sites, as

$$\tilde{g} = \frac{g_2 g_3}{h_2}. \quad (42)$$

Comparing the decimation equations in Eqs. (41) and (42) with those for the random contact process in Eqs. (19) and (21) we can see that they are equivalent. This is not surprising, since the two Hamilton operators in Eqs. (18) and (40) are related through a unitary transformation [3], if  $\mu_i \leftrightarrow h_i$  and  $\lambda_i \leftrightarrow g_i$ . Consequently the singular behavior of the random contact process and the random Reggeon field theory are equivalent.

Next, we consider the geometrical interpretation of directed percolation and study its critical behavior in the very strong disorder limit.

#### 2. Strong disorder: Mapping to random walks

Here we consider directed percolation on the square lattice with random occupation probabilities which are, however, strictly correlated in the same layer, as shown in Fig. 1.

For simplicity, we use a bimodal distribution, the occupation probability in the  $i$ -th layer can be either  $p_i = q$  with

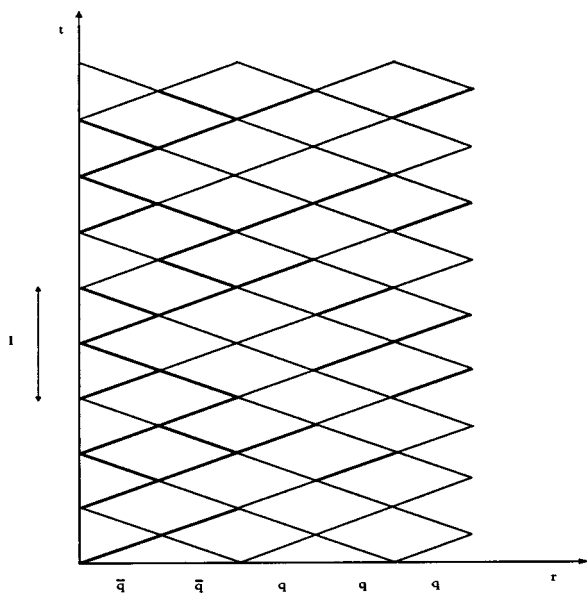


FIG. 1. Directed percolation on the square lattice with random bond occupation probabilities, which are perfectly correlated along the vertical diagonal direction. Occupied bonds are drawn in bold. In the two columns on the left bonds are occupied with a large probability  $\bar{q}$ , while in the other three columns this probability is small and equals  $q$ . The typical length-scale in the problem is  $l \sim 1/q$ . The direction of time,  $t$ , is also indicated which gives a reinterpretation of directed percolation in terms of a reaction-diffusion model.

probability  $\pi$  or  $p_i = 1 - q = \bar{q}$ , with probability  $\bar{\pi}$  (we take  $q \leq \bar{q}$ ). For isotropic percolation the critical point is located at  $\pi = \bar{\pi} = 1/2$ , which follows from self-duality [43]. Since directed clusters generally contain less bonds than the isotropic ones, for directed percolation at the critical point  $\pi < \bar{\pi}$ . In the strong disorder limit we take  $q \rightarrow 0$  in which case at the critical point  $(\pi/\bar{\pi})_c \rightarrow 1$  as we shall show below. The effect of the same type of disorder for isotropic percolation has already been considered by one of us [43]. The reasonings in the two problems are very similar and they lead to identical critical properties. Therefore, here we just briefly describe the method and emphasize the relations and differences between the directed and isotropic problems. For more details we refer to the original Ref. [43].

The characteristic structure of the occupied bonds is very different for the two types of layers. In layers with a large probability,  $p_i = \bar{q}$ , almost all bonds are occupied, between two unoccupied bonds there is a characteristic distance,  $l \sim 1/q$ . On the other hand in layers with a small probability,  $p_i = q$ , there are only very few occupied bonds; two occupied bonds are separated by the same characteristic distance,  $l \sim 1/q$ . Note the duality: for layers with  $p_i = q$  the nonoccupied (say white) bonds play the same role as the occupied (say black) bonds for layers with  $p_i = \bar{q}$ .

Now let us consider a system consisting of  $r = 1, 2, \dots, L$  layers with free boundary conditions, with the seed at  $r = 0$  and determine the surface order-parameter,  $\rho_s(L)$ , which is given by the probability that the percolating cluster extends up to the other surface at  $r = L$ . To calculate  $\rho_s(L)$  we consider strips of width  $k = 1, 2, \dots, L$  and estimate,  $n(k)$ , the

typical number of sites in the  $k$ -th (i.e., surface) layer which are connected to the seed. It is evident from the duality properties that for  $n(k) \gg 1$  the probability that the seed is connected to the  $k$ -th layer through *white* bonds is  $p_w(k) \sim 1/n(k)$ , since typically one out of  $n(k)$  sites has this property. We show by induction that  $n(k)$  is either zero or given by  $n(k) \sim q^{-X(k)}$ , where  $X(k) > 0$  is the number of layers with a probability  $\bar{q}$  minus the number of layers with a probability  $q$ . First, our statement is trivially true for  $k = 1$ . Here  $n(1) \sim 1/2q$  [and thus  $p_w(k) \sim q$ ], for  $p_1 = \bar{q}$  and  $n(1) = 0$ , for  $p_1 = q$ . Evidently, if in a given sample  $n(k) = 0$  for some  $k < L$ , then  $n(k') = 0$  for any  $k' > k$  and the surface order-parameter is zero. To complete our proof, in the second step we show that, if  $X(k) \geq 1$ , then  $X(k+1) = X(k) \pm 1$ , where the upper (lower) sign stands for a probability  $p_{k+1} = \bar{q}$  ( $p_{k+1} = q$ ). The proof of this statement follows from the fact that for  $p_{k+1} = q$  the number of black bonds in the cluster at layer  $k$  is reduced by a factor of  $\sim q$ , whereas for  $p_{k+1} = \bar{q}$  the probability  $p_w(k)$  is reduced by a same factor  $\sim q$ . Here, when  $X(k) = 1$  and  $p_{k+1} = q$ , thus  $X(k+1) = 0$  the cluster is considered to be terminated at this point; thus  $\rho_s(L) = 0$ .

To calculate the average value of the surface order-parameter we use a random walk picture, which has already been applied in the isotropic problem [43]. To a given sample with a given probability distribution we assign a random walk which starts at position  $X_0 = 0$  and makes its  $i$ -th step upwards (downwards) for  $p_i = \bar{q}$  ( $p_i = q$ ). The position of the walker in the  $k$ -th step is just  $X_k$ . The existence of the finite surface order-parameter in the given sample is then formulated by the condition  $n(k) > 0$  for  $k = 1, 2, \dots, L$ ; thus  $X_k > 0$  for  $k = 1, 2, \dots, L$  so that the random walk has a surviving character. The average *value* of the surface order-parameter is given by the fraction of samples with finite surface order, which is just the survival probability of the random walk:  $[\rho_s]_{\text{av}}(L) \sim P_s(L) \sim L^{-1/2}$ . From this relation the value of the surface order-parameter scaling dimension,  $x_s = 1/2$  follows, which is the same as for the random contact process in the strong disorder fixed point in Eq. (39). Note that the rare events introduced in Sec. II B in this case are the samples with a surviving characteristics in the probability distribution. Furthermore in the critical situation, when the average surface order-parameter decays as a power with  $L$  the probabilities,  $\pi = \bar{\pi}$ , as announced before.

Other exponents can be deduced in an analogous way as for isotropic percolation. The typical temporal extent of the percolating cluster is given by the typical number of connected sites in a layer,  $\xi_{\parallel} \sim n_{\text{typ}}(L) \sim q^{-X_{\text{typ}}}$ , where the typical excursion of a (surviving) random walk in  $L$  steps is  $X_{\text{typ}} \sim L^{1/2}$ . Thus we have the logarithmic scaling relation in Eq. (8) with  $\psi = 1/2$ , as for the random contact process. To calculate the bulk order-parameter the seed is put in the middle of the lattice and in a given sample  $\rho(L) = O(1)$  if the percolating cluster has an extent of  $L$ . In the language of random walks this property is related to the so called average persistence [44]. From this, scaling of the average (bulk) order-parameter is given by  $[\rho]_{\text{av}}(L) \sim L^{-x}$ , with  $x = (3 - \sqrt{5})/4$ , as for the random contact process in Eq. (37). Finally, to determine the scaling exponent of the order-parameter in the vicinity of the critical point one should consider random walks



with finite bias,  $\delta_w \neq 0$ , towards the absorbing walk and  $\delta \sim \delta_w$ . From the scaling of the surviving probability of biased walks [34] one obtains for the correlation length,  $\xi_\perp \sim |\delta|^{-2}$ . Thus we recover the same exponent,  $\nu_\perp = 2$ , as for the random contact process in Eq. (34).

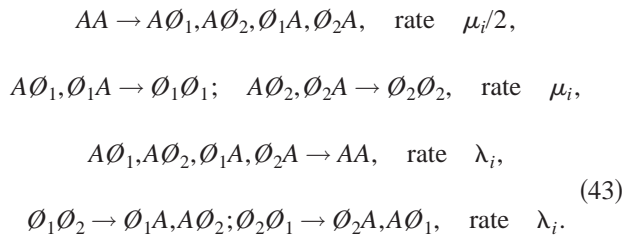
Hence we can conclude that the critical properties of random directed percolation can be deduced from a random walk mapping in the strong disorder limit. The critical behavior is the same as for random isotropic percolation and corresponds to the RG results obtained for the random contact process in the strong disorder fixed point.

### C. The generalized contact process with disorder

So far we have considered different variants of absorbing state phase transitions which, in the absence of disorder, all belong to the directed percolation universality class. We observed that in the presence of strong enough quenched disorder all these processes show strong disorder scaling behavior with identical critical exponents. In this section we consider other processes, which are not in the directed percolation universality class.

For a renormalization group treatment, one of the most convenient models is the generalized contact process with several different absorbing states introduced by Hinrichsen [8]. In this model a site can be occupied by a particle,  $A$ , or can be in one of  $n$  empty states  $\emptyset_1, \emptyset_2, \dots, \emptyset_n$ . Furthermore, besides the rules known for the ordinary contact process, there is a competition between the different type of empty states. At the border of clusters with a different type of empty states, particles can be created. As a consequence, in these models, with increasing  $n$  there is a preference for the active phase and the phase transitions is found to be in universality classes different from the directed percolation one. For  $n = 2$ , the model was shown to be in the parity conserving class [8], whereas for  $n \geq 3$  the model is always active [45].

Here we consider in particular the effect of a disorder on the model with  $n=2$ . For this case, the following processes are allowed:



For nonrandom couplings the phase-transition in one dimension is located at  $\mu/\lambda = 1.592$  and the critical exponents are  $\nu_\perp = 1.82$ ,  $z = 1.75$ ,  $\beta = 0.91$  consistent with those of the parity conserving universality class. Note that the Harris-type criterion in Eq. (1) with the above  $\nu_\perp$  predicts a relevant perturbation for quenched disorder.

Next, for the random system we try to apply the renormalization group method along the lines used for the random contact process in Sec. III A. We start with the decimation scheme and consider the situation when the largest rate is a branching rate, say  $\lambda_2 = \Omega$ . As for the random contact process we take the two-site Hamiltonian, which contains now 9

states, since each site could be in three (one active and two different inactive) states, and calculate the lowest three eigenstates along the lines presented in Appendix A for the random contact process. Among the three lowest states, which are kept after decimation, two have eigenvalues, 0, and the third has an energy  $\epsilon_1^{23} \approx 2\mu_2\mu_3/\lambda_2$ . Thus after decimation we have an effective two-site cluster in the presence of a renormalized death rate, which is given just in the same form as in the random contact process; see Eq. (19). The value of the effective death rate can be also obtained by a similar argument as for the random contact process. In order to calculate the decay from  $AA \rightarrow \emptyset_1\emptyset_1, \emptyset_2\emptyset_2$  one should consider two second-order virtual processes:  $AA \rightarrow A\emptyset_1 \rightarrow \emptyset_1\emptyset_1$  and  $AA \rightarrow \emptyset_2 \rightarrow \emptyset_2\emptyset_2$ , which leads to Eq. (19) by taking into account the definition of the rates in Eq. (43).

For the case of a strong elimination rate,  $\mu_2 = \Omega$ , the three-site Hamiltonian contains 27 eigenstates, which are divided into 9 orthogonal sectors, each of which have 3 states. The highest levels of each sector have an energy of  $O(\mu_2)$  and thus can be discarded during decimation. The remaining 18 states, however, are all in the same order of magnitude. Three sectors have ground state energy zero and first excitation energy,  $\lambda_2 + \lambda_3$ . Two other sectors have the lowest energies:

$$\epsilon_2^{123} = [(7\lambda_2 + 4\lambda_3) \pm \sqrt{(7\lambda_2 + 4\lambda_3)^2 - 16\lambda_2\lambda_3}]/8, \tag{44}$$

and in another two we should exchange in Eq. (44),  $\lambda_2$  and  $\lambda_3$ . Finally the last two sectors are also degenerate with the lowest eigenvalues:

$$\epsilon_3^{123} = [3(\lambda_2 + \lambda_3) \pm \sqrt{9(\lambda_2 + \lambda_3)^2 - 32\lambda_2\lambda_3}]/4. \tag{45}$$

Consequently the decimation does not work out here for a large death rate, since (i) one can only discard 9 out of the 27 cell states, so that the remaining states cannot be assigned to one renormalized site and (ii) the remaining energy levels are of the same order as the original rates; thus the energy scale is not lowered during these steps. These features of the decimation can be seen by the following argument, too. With a large death rate,  $\mu_2 = \Omega$ , the site  $i=2$  is almost always inactive, so that it is either in  $\emptyset_1$  or  $\emptyset_2$  most of the time. Suppose we decimate this site and calculate the effective rate for a process in which in the original lattice at sites 1 and 3 there is  $A$  and  $\emptyset_1$ , respectively, which will change to  $A$  and  $A$ . In the original bases this process can most easily be realized through  $A|\emptyset_2|\emptyset_1 \rightarrow A|\emptyset_2|A$ , which (i) has a rate  $\lambda_2$  and (ii) the effective rate does not depend on the fact that site 1 is occupied. Consequently during renormalization new degrees of freedom will appear and there is no systematic decrease of the energy-scale.

Thus we can conclude that the renormalization group scheme does not work for the generalized contact process. Therefore, it is improbable that a strong disorder fixed point with the scaling properties described in Sec. II B could be present in this model for some finite value of the disorder. The qualitative difference between the random contact process and the generalized random contact process is due to the competition between the different absorbing states in the latter model. For this case a large death rate indirectly promotes

particle branching, since the active phase intrudes between the different absorbing states. This is the reason why the pure model is always in the active phase for  $n \geq 3$  [45]. This could also be true for the random model.

#### IV. NUMERICAL INVESTIGATIONS

Here, we discuss the results of two numerical approaches which allow us to investigate the disordered contact process as a function of disorder strength. In this way, we will be able to show that the predictions made in the previous section are consistent with the numerical results provided the disorder is strong enough. However, we also find that there is a regime at small to intermediate disorder in which the critical exponents deviate from the strong disorder ones and indeed seem to vary continuously. This is evidence for a line of fixed points. However, the numerical results available do not allow us to decide whether these are ordinary disorder fixed points (finite  $z$ ) or strong disorder ones (infinite  $z$ ).

##### A. One-dimensional random contact process

In our numerical work, we investigated the particular case for which the rate  $\mu_i=1$  and the branching rate  $\lambda_i$  is distributed according to

$$R(\lambda) = [\delta(\lambda - \lambda_+) + \delta(\lambda - \lambda_-)]/2, \quad (46)$$

with  $\lambda_{\pm} = \exp(A \pm \sqrt{D})$ . The main advantage of this distribution is that it allows an exact average over the disorder to be made, at least on lattices that are not too large. For this choice of  $R(\lambda)$  the average value of  $\ln \lambda$  equals  $A$  whereas the variance is  $D$ . These can therefore be considered as suitable parameters to measure the activity and the disorder, respectively.

##### 1. DMRG studies

The density matrix renormalization group (DMRG) method is a numerical technique that was originally introduced to investigate the properties of quantum spin or fermion systems. The method allows a precise determination of the properties (energy, magnetization profiles, correlations, ...) of the ground state and low lying excitations of such models. The method is most successful in one dimension. Given the formal similarity between quantum systems and stochastic ones, several groups started to apply this technique to interacting particle systems in recent years [23,45]. The method is now known to work well also in these cases though it cannot give as accurate results as for the spin chains, mainly because at this moment algorithms to diagonalize non-Hermitian matrices are not as well developed as those for the Hermitian case.

In our DMRG work we made calculations for systems with up to  $L=24$  sites. For  $L \leq 14$  we were able to perform an exact average over all possible realizations of the disorder. For the larger systems sizes we considered typically around  $10^4$  disorder realizations. These calculations were possible for  $D \leq 2$ . For larger  $D$ -values, we encountered numerical difficulties in the DMRG algorithm.

In any finite system, the stationary state of the contact process is the absorbing state, i.e., the lattice without any particles. In order to study the absorbing state phase transition within finite systems, we therefore worked with open boundaries and put the death rate at the most right site of the lattice,  $\mu_L$ , equal to zero. This ensures the presence of particles in the stationary state. It can be expected that for large enough systems and for sites that are deep in the bulk the effect of this boundary will be negligible.

Using the DMRG we then first calculated the ground state of the generator (18) with open boundaries. Within this ground state we calculated the density profile, i.e.  $\rho_i = [\langle n_i \rangle]_{\text{av}}$ .

In order to determine the location of the critical point and the critical exponents  $x$ ,  $x_s$ , and  $\nu_{\perp}$  we investigated in detail the behavior of  $\rho_s = \rho_1$  (surface density) and  $\rho_{L/2}$  (which we took as our estimate for the bulk density) as a function of the parameters  $A$  and  $D$ .

A major problem of the contact process in comparison with several well studied disordered quantum spin chains is that in the present case the location of the critical point is not known exactly. The numerical inaccuracy in the location of the critical point will in its turn influence the accuracy by which critical exponents can be determined.

To locate the critical point we investigated the quantity

$$Y_L = \frac{d \ln \frac{d\rho}{dL}}{d \ln L}. \quad (47)$$

For a homogeneous system,  $\rho$  reaches its large  $L$ -value exponentially fast away from the critical point, and as a power law at the critical point [see (2) and (3) which are the same in the stationary state]. As a consequence  $Y_L$  goes to  $-\infty$  for a noncritical system and to  $-(1+x)$  at criticality. We can therefore expect that in a finite system, the quantity  $Y_L$  goes through a maximum as a function of  $\mu/\lambda$  from which one can obtain a finite size estimate of the location of the critical point and of  $x$ . In this way we have obtained the critical value of  $A$ , denoted as  $A_c$  for different values of the disorder strength  $D$  and for different  $L$ -values. An extrapolation for  $L \rightarrow \infty$  then gives our final estimates for  $A_c(D)$ . The data for the surface density  $\rho_s$  can be analyzed in a completely similar way and give an independent estimate for the location of the critical point. From the analysis in Sec. II, we expect that for  $D \rightarrow \infty$ , the critical point obeys  $[\ln \mu]_{\text{av}} = [\ln J]_{\text{av}}$  which for the present case leads to the prediction of the exact location of the critical point, at  $A_c = \ln \sqrt{8} = 1.0397$ . Unfortunately, we are not able to investigate very large  $D$ -values and hence could not verify this prediction.

To determine the stationary state critical exponents we next made scaling plots for the density and the surface density assuming (2) (taking  $t \rightarrow \infty$ ). In Fig. 2 we show such a scaling plot for the density and for  $D=0.25$  and  $A_c=1.19$ . From this we obtain  $x=0.24$  and  $\nu_{\perp}=1.25$ . Data for the bulk and surface density for other values of  $D$  can be analyzed in a completely similar way and they give rise to the DMRG estimates for the exponents  $x_s$  and  $x$  as shown in Fig. 3 of Ref. [31] and Fig. 6, respectively. From these we see that  $x_s$

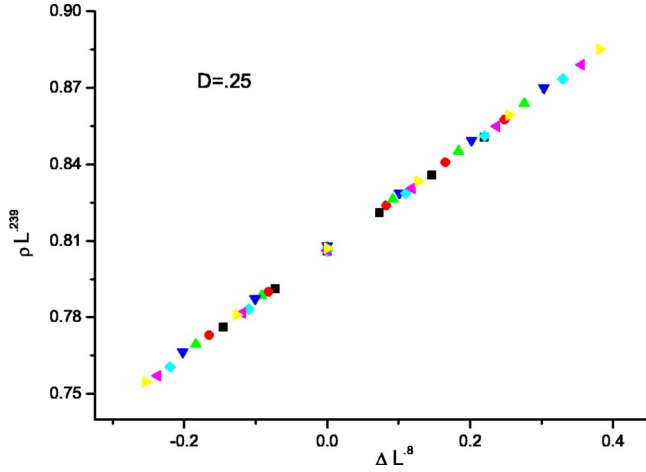


FIG. 2. Scaling plot of the particle density at  $D=0.25$  assuming  $A_c=1.19$ ,  $x=0.24$ , and  $\nu_{\perp}=1.25$ . The different symbols indicate  $L=12(\square)$ ,  $L=14(\circ)$ ,  $L=16(\triangle)$ ,  $L=18(\nabla)$ ,  $L=20(\diamond)$ ,  $L=22(\triangleleft)$ , and  $L=24(\triangleright)$ .

assumes the value predicted for the strong disorder fixed point at  $D \geq 1.5$ . For smaller  $D$ -values,  $x_s$  decreases continuously starting from its value for a homogeneous contact process ( $x_s \approx 0.669$  [32]).

A rather similar behavior is found for the bulk exponent  $x$ . For increasing  $D$ , its value decreases from that for the homogeneous contact process,  $x \approx 0.252$ , to a value of  $x \approx 0.2$  in the region  $1.5 \leq D \leq 2$ . Here it has to be remarked that since the DMRG can only be performed for systems with  $L$  up to 24, it may very well be that our estimate of the bulk density  $\rho$  is still influenced by the boundary conditions which we had to choose, and this may very well be the reason why the exponent  $x$  reaches its value at the strong disorder fixed point more slowly.

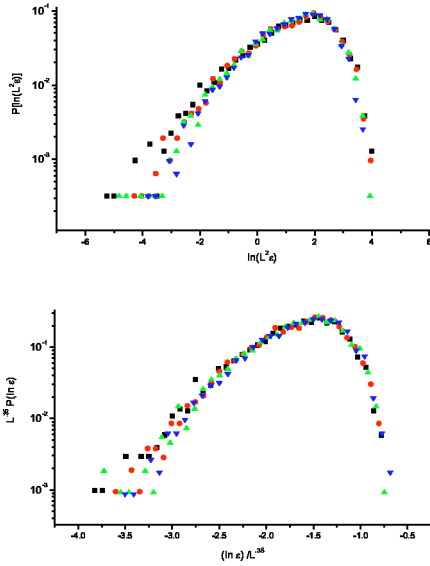


FIG. 3. Test of dynamical scaling form for  $D=0.5$ ,  $A_c=1.19$ . In the upper graph, we have assumed ordinary dynamical scaling with  $z=2.0$ , while in the lower graph we used logarithmic scaling with  $\psi=0.35$ . The different symbols correspond with  $L=18(\nabla)$ ,  $L=20(\triangle)$ ,  $L=22(\circ)$ , and  $L=24(\square)$ .

The exponent  $\nu_{\perp}$  is even more difficult to estimate since its value is very sensitive to the precise location of the critical point. The values that we have determined are only rough estimates. We find that the value of  $\nu_{\perp}$  increases from the pure system value with increasing disorder, and equals  $1.67 \pm 0.08$  at  $D=1.5$ .

The exponent  $z$ , or in case of a logarithmic scaling  $\psi$ , can in principle be determined from the distribution of the gap in the spectrum of the generator (18). Using the DMRG, we therefore also calculated the distribution of gap sizes for different system sizes. In Fig. 3 we show the results of such an analysis at the critical point and for  $D=0.5$ . In the upper graph we show a plot assuming ordinary scaling and the value  $z=2$ , while in the lower part we have assumed logarithmic scaling and  $\psi=0.35$ . As can be seen from this figure, the DMRG-results do not allow us to discriminate between the two types of dynamical scaling. A similar conclusion holds for other  $D$ -values.

2. Monte Carlo simulations

In an attempt to reach bigger system sizes and to get independent estimates for the exponents we also performed extensive numerical simulations taking a single seed particle as an initial condition. In order to have a good comparison with DMRG-data, we again put all death rates equal to one, while the branching rates are distributed according to (46). For various values of  $D$  and  $A$  we calculated the survival probability  $P_s(t)$ , the total number of particles in the system  $N(t)$  as well as their average spread  $R^2(t)$ . We typically simulated up to  $t=10^5$  and took an average over  $2 \times 10^4$  disorder realizations. For each of these realizations we simulated one history of the stochastic process. In performing the simulations starting from one seed particle at time  $t=0$ , there can be at most  $2t+1$  occupied sites in the lattice after time  $t$ . In our simulations the size of the system grows with time to take account of this. So in fact, we can say that we simulate an infinite system, at least for the particular initial conditions chosen. For large  $D$ -values, it is difficult to obtain reliable simulation data since the dynamics becomes extremely slow. For this reason we are not able to explore values of  $D$  that are much larger than  $\approx 1.5$ .

To analyze our data we first have to determine the location of the critical point  $A_c(D)$ . While in homogeneous systems the critical point is the only one characterized by a power law decay of  $P_s(t)$ , the same is not true in a disordered system as first pointed out by Bramson, Durrett, and Schonmann [17]. Power law behavior can indeed be found in the whole subcritical regime and is a manifestation of the presence of a Griffiths phase. Still, we expect  $N(t)$  to increase above  $A_c$  and to decrease below criticality. In this way we obtain a first estimate of the location of the critical point. A second criterion which we used is that both for conventional and for strong disorder scaling, at criticality,  $\ln P / \ln N$  becomes a constant asymptotically. In Fig. 4 we show a typical set of data for this quantity taken at  $D=0.5$ . From these we determine  $A_c(0.5)=1.177$ . The values for the critical activities which we find in this way are close (approximately within 1%) to these found from the DMRG.

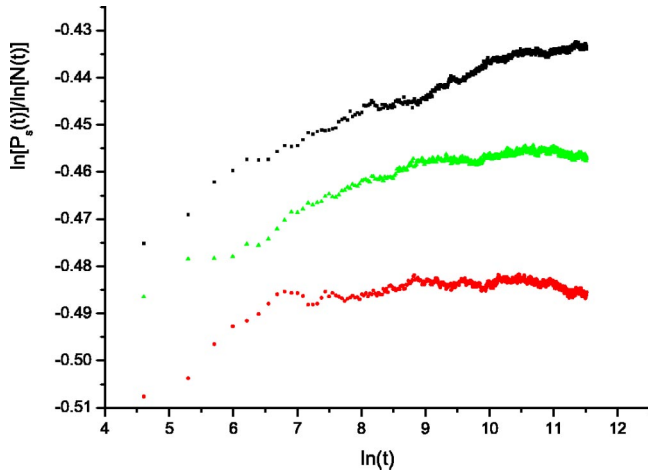


FIG. 4. Plots of  $\ln P_s(t)/\ln N(t)$  as a function of  $\ln t$  at  $D=0.5$  and for  $A=1.179, 1.177,$  and  $1.175$  (top to bottom). From this, we estimate  $A_c=1.177$ .

In Fig. 5 we present log-log plots for the three quantities of interest at the critical point with  $D=1$ . These results are typical also for the other  $D$ -values investigated.

As can be seen there is still some curvature visible in these figures, which could e.g. arise from the logarithmic corrections which are ubiquitously present in these kind of random “quantum” systems. Yet, the late time part can be fitted quite well to a power law from which we can determine estimates of the exponents  $x$  and  $z$  as a function of  $D$ .

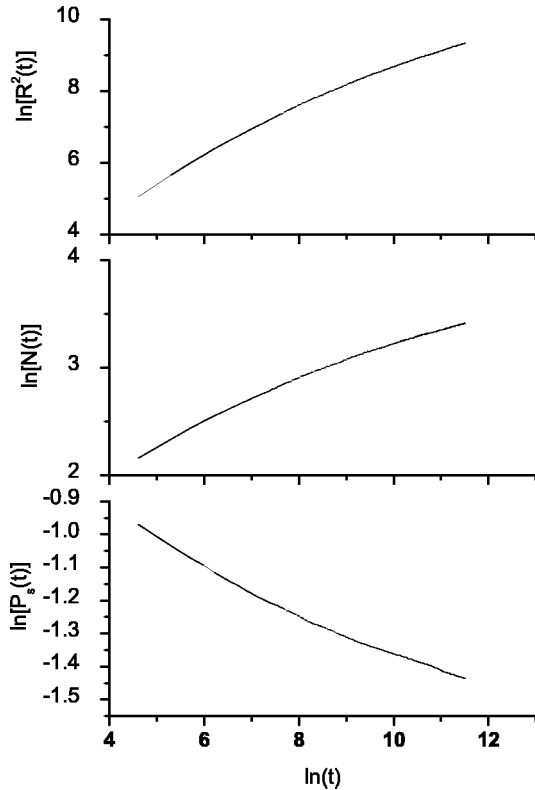


FIG. 5. A plot of the survival probability  $P_s(t)$ , the number of particles  $N(t)$  and their average spread  $R^2(t)$  (bottom to top) as a function of  $t$  for  $D=1, A_c=1.171$ .

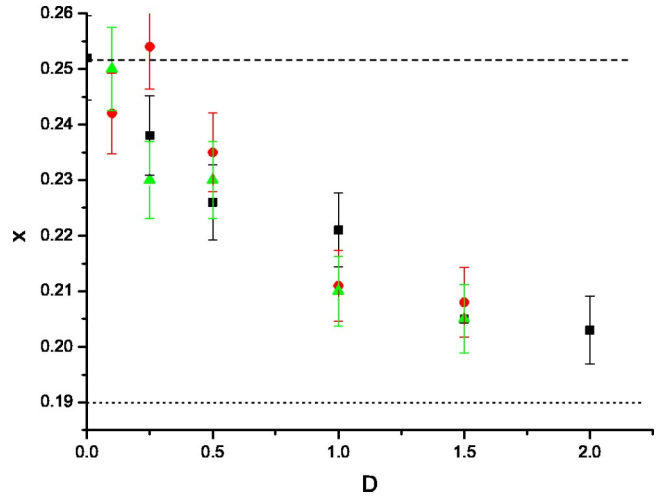


FIG. 6. A plot of the exponent  $x$  versus disorder strength  $D$ . The different symbols indicate the results obtained from the DMRG (squares), and the simulations assuming ordinary scaling (circles) and logarithmic scaling (triangles). We also indicate the values for strong disorder (dotted line) and for the homogeneous system (dashed line).

Our results for these exponents are presented in Figs. 6 and 7, respectively.

We notice two interesting trends. First, we observe a decrease of  $x$  from its homogenous system value to a value that is consistent with that at the infinite disorder fixed point. The numerical values are moreover consistent with those found from the DMRG. Second, we observe that the dynamical exponent  $z$  seems to make a jump as soon as any disorder is present after which it increases with  $D$ . These results are then consistent with the idea of a line of ordinary (disorder) critical points which ends at some critical value of the disorder above which exponents assume precisely the values of the strong disorder fixed point.

In a regime governed by strong disorder fixed points we expect that the dynamical quantities do not follow a power law but scale logarithmically, i.e., as given in (13). Indeed such a behavior was found in the simulations in  $d=2$ . [15] We found that this kind of scaling can also describe our

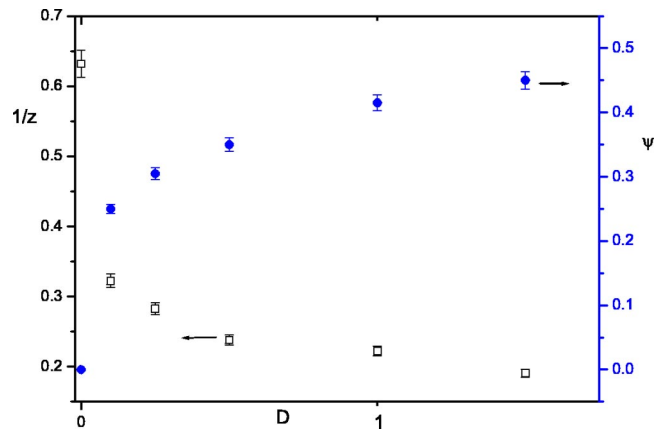


FIG. 7. A plot of the exponents  $1/z$  (squares) and  $\psi$  (circles) as a function of disorder strength  $D$ .



results for all  $D$ -values investigated. Assuming strong disorder scaling, we can determine estimates for the exponents  $x$  and  $\psi$ . These values are also shown in Figs. 6 and 7. We notice that the values for the exponent  $x$  are not very sensitive to the type of scaling that we assumed. We also observe that the exponent  $\psi$  seems to increase towards its value expected at the strong disorder fixed point, i.e.  $\psi=1/2$ .

We can thus see that, as was for the case for the DMRG, it is not possible to rule out from the numerics that there is a line of strong disorder fixed points in the model. When we compare the estimates for the dynamical exponents coming from the two numerical approaches, we find that those for the logarithmic corrections are more self-consistent. There is a rather large discrepancy between the  $z$ -values as found from the DMRG and the simulations. This could be due to a lack of asymptoticity in time for the simulations and in size for the DMRG. Assuming logarithmic scaling, the values which we find from the two approaches are almost the same. The existence of a line of strong disorder fixed points was not found so far in real quantum systems and could be an essential new feature of stochastic models. Yet, at present we have no theoretical underpinning for the existence of such a line of disorder fixed points. Further numerical studies are needed to obtain more insight on this point.

### B. Two-dimensional random contact process

As already remarked above, in the second paper of Ref. [15], the logarithmic scaling (13) was first observed in the two-dimensional contact process with dilution where it was dubbed “violation of scaling.” In the present work we have shown that this kind of scaling is the natural one to be expected at a strong disorder fixed point. In Ref. [15] it was assumed that the logarithmic scaling holds for all values of the dilution, which here we will denote by  $p$ . Since we do not have the original dataset, it is not possible to investigate whether the data of these authors are also consistent with ordinary scaling in the small  $p$ -regime. From the numerically determined values of  $\bar{\theta}$ ,  $\bar{\eta}$ , and  $\bar{\sigma}$  it is however possible to determine values for the exponents  $x$  and  $\psi$  in the two-dimensional case. The results are shown in Fig. 8.

These numbers can now be compared with those expected to hold at the strong disorder fixed point of the RTIM in two dimensions, which are  $x=1.0$  and  $\psi=0.42$ . Note that for the largest disorder value, the exponent  $\psi$  is very close to this value. The exponent  $x$  seems larger than expected. However, in this respect it is interesting to remark that the authors of Ref. [15] notice that the data on  $N(t)$  are consistent with ordinary scaling but with  $\eta=0$  or with logarithmic scaling and a very small value of  $\bar{\eta}$ . This is consistent with our ideas which predict that at the strong disorder fixed point in  $d=2$  and for  $x=1$ ,  $\bar{\eta}$  equals zero. Hence, we believe that also in two dimensions the strongly disordered contact process is in the same universality class as the RTIM.

## V. CONCLUSIONS

In this paper, we have investigated the effect of quenched disorder in the transition rates on the critical behavior of

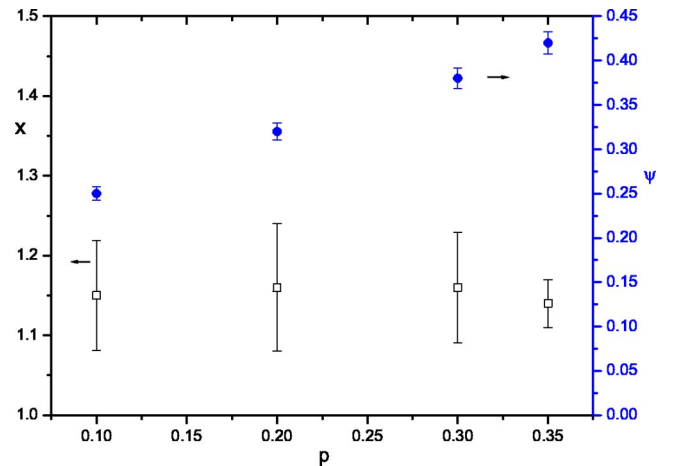


FIG. 8. Values for the exponents  $x$ (squares) and  $\psi$ (circles) as a function of dilution  $p$  assuming logarithmic scaling. The values in this table are for  $d=2$  and are determined from the numbers given in Table I of the first paper in Ref. [15].

some models with absorbing state phase transitions. For models in the directed percolation universality class, we have given convincing evidence that, if the disorder is large enough, the universal behavior is that known from the RTIM and some other disordered quantum spin chains. This result follows from calculations using a strong disorder renormalization approach and is consistent with numerical results in one dimension obtained with the DMRG and simulations. A reanalysis of data for a diluted contacted process in two dimensions is also consistent with this conclusion. It therefore seems that the effects of strong disorder lead to a new kind of universality between Hermitian and non-Hermitian quantum models.

For a weak and intermediate disorder our numerical results indicate the existence of a line of fixed points with continuously varying exponents. Such behavior has been found previously in some quantum spin chains [46]. Most interestingly, our data could be consistent with a scenario in which this is a line of strong disorder fixed points. Such a behavior is also consistent with data obtained by Moreira and Dickman on a two-dimensional diluted contact process. Further simulations are needed to confirm this picture. It would be especially interesting to develop techniques that can efficiently simulate these kinds of systems for sufficiently large disorder and long enough times. Moreover, it would be very interesting to investigate whether the behavior that we find can also be seen for distributions of the transition rates different from the ones that we used in our simulations. If the logarithmic dynamical behavior can be demonstrated, it becomes a challenge to understand such behavior from analytical or RG arguments.

For absorbing state phase transitions in other universality classes we have fewer results. Our RG calculations indicate that for the generalized contact process with disorder, it may be possible that the model is always active, also for  $n=2$ . This prediction should be verifiable with simulations. Whether this result also holds for other models in the same universality class is not clear yet. We believe that the effect of quenched disorder on absorbing state phase transitions in

particular, and on stochastic many-particle systems in general, provides an interesting field of future research.

### ACKNOWLEDGMENTS

J.H. is thankful to G.T. Barkema for useful discussions concerning the simulations. F.I. is grateful to P. Grassberger, J.D. Noh, and F. van Wijland for stimulating discussions and to L. Gránásy for his help in the numerical calculations. F.I.'s work has been supported by the Hungarian National Research Fund under Grant No OTKA TO34183, TO37323, MO28418 and M36803, by the Ministry of Education under Grant No. FKFP 87/2001, by the EC Centre of Excellence (No. ICA1-CT-2000-70029) and the numerical calculations by NIIF 1030. In the early stages of this work, J.H. was supported by the FWO-Vlaanderen.

### APPENDIX A: DECIMATION FOR THE RANDOM CONTACT PROCESS

When the branching rate between two sites (say 2 and 3) is the largest rate in the system, we consider the Hamiltonian (18) restricted to these two sites and with free boundary con-

ditions. This operator can be represented by the matrix

$$\mathbf{H}_{CP}^{23} = \begin{pmatrix} 0 & -\mu_3 & -\mu_2 & 0 \\ 0 & \mu_3 + \lambda_2 & 0 & -\mu_2 \\ 0 & 0 & \mu_2 + \lambda_2 & -\mu_3 \\ 0 & -\lambda_2 & -\lambda_2 & \mu_2 + \mu_3 \end{pmatrix}. \quad (\text{A1})$$

In the limit  $\mu_2/\lambda_2 \rightarrow 0$  and  $\mu_3/\lambda_2 \rightarrow 0$  the eigenvalues are 0, 0,  $\lambda_2$ ,  $\lambda_2$ . The degeneracies disappear for finite  $\mu_2/\lambda_2$  and  $\mu_3/\lambda_2$ . Discarding the two highest energy levels, the gap between the remaining two lowest states can be calculated perturbatively leading to

$$E_{CP}^{23} = \frac{2\mu_2\mu_3}{\lambda_2}. \quad (\text{A2})$$

Now keeping in mind that a one-site cluster with a death rate  $\tilde{\mu}$  has a gap  $\tilde{\mu}$  we obtain for the renormalized death rate,  $\tilde{\mu}_2 = E_{CP}^{23}$ , as announced in (19).

When the largest rate is a death rate, say  $\mu_2$ , one considers a three site cluster whose Hamiltonian (free boundary conditions) is represented by the matrix

$$\mathbf{H}_{CP}^{123} = \begin{pmatrix} 0 & -\mu_2 & 0 & 0 & 0 & 0 & 0 & 0 \\ 0 & \mu_2 + \lambda_2 + \lambda_3 & 0 & 0 & 0 & 0 & 0 & 0 \\ 0 & 0 & \lambda_2 & -\mu_2 & 0 & 0 & 0 & 0 \\ 0 & -\lambda_2 & -\lambda_2 & \mu_2 + \lambda_3 & 0 & 0 & 0 & 0 \\ 0 & 0 & 0 & 0 & \lambda_3 & -\mu_2 & 0 & 0 \\ 0 & -\lambda_3 & 0 & 0 & -\lambda_3 & \mu_2 + \lambda_2 & 0 & 0 \\ 0 & 0 & 0 & 0 & 0 & 0 & \lambda_2 + \lambda_3 & -\mu_2 \\ 0 & 0 & 0 & -\lambda_3 & 0 & -\lambda_2 & -\lambda_2 - \lambda_3 & \mu_2 \end{pmatrix}. \quad (\text{A3})$$

The corresponding eigenvalue problem is reduced to the diagonalization of four  $2 \times 2$  matrices. In each subspace there is an eigenvalue of  $O(\mu_2)$ , which is discarded. Of the remaining four lowest eigenvalues there are two zero and two with the value

$$E_{CP}^{123} = \frac{\lambda_2\lambda_3}{\mu_2}. \quad (\text{A4})$$

If we keep in mind that in a two-site cluster with an effective branching rate  $\tilde{\lambda}$  the spectrum is given by 0, 0,  $\tilde{\lambda}$ ,  $\tilde{\lambda}$  we obtain for the renormalized rate  $\tilde{\lambda} = E_{CP}^{123}$  the result stated in (21).

### APPENDIX B: SOLUTION OF THE RG EQUATIONS AT THE CRITICAL POINT

We look for a special solution of (25) and (26) (in the fixed point  $\Omega \rightarrow 0$ ) of the form

$$R(J, \Omega) = R(\Omega, \Omega) \left( \frac{\Omega}{J} \right)^{1-R(\Omega, \Omega)\Omega}, \quad (\text{B1})$$

$$P(\mu, \Omega) = P(\Omega, \Omega) \left( \frac{\Omega}{\mu} \right)^{1-P(\Omega, \Omega)\Omega}. \quad (\text{B2})$$

Substituting (B1) and (B2) into (25) we get

$$\frac{d \ln \tilde{R}}{d\Omega} - \frac{d\Omega \tilde{R}}{d\Omega} \ln \frac{\Omega}{J} + \frac{1 - \Omega \tilde{R}}{\Omega} = \tilde{P} - \tilde{R} - \Omega \tilde{R} \tilde{P} \ln \frac{\Omega \kappa}{J} \kappa^{-\Omega \tilde{R}}, \quad (\text{B3})$$

where we used the notations  $\tilde{P}(\Omega) \equiv P(\Omega, \Omega)$  and  $\tilde{R}(\Omega) \equiv R(\Omega, \Omega)$ . For a moment we set  $\kappa = 1$ . After a trivial rearrangement, we obtain the relation

$$\left[ \Omega \tilde{R} \tilde{P} - \frac{d\Omega \tilde{R}}{d\Omega} \right] \left[ \ln \frac{\Omega}{J} - \frac{1}{\Omega \tilde{R}} \right] = 0, \quad (\text{B4})$$

which leads to the ordinary differential equations

$$\frac{d\tilde{R}}{d\Omega} = -\frac{\tilde{R}}{\Omega} + \tilde{P}\tilde{R}, \quad (\text{B5})$$

$$\frac{d\tilde{P}}{d\Omega} = -\frac{\tilde{P}}{\Omega} + \tilde{P}\tilde{R}. \quad (\text{B6})$$

These equations which hold just for  $\kappa=1$  can be solved for general (nonsymmetric) distributions [39]. The solution gives information about the singular behavior of the system outside the critical point, i.e., in the Griffiths phase. This general solution, however, does not apply for  $\kappa \neq 1$ . On the contrary, the solution at the fixed point, when  $R(J, \Omega)$  and  $P(\mu, \Omega)$  are identical, thus  $\tilde{R}=\tilde{P}$ , holds for any finite  $\kappa > 0$ . Indeed, in terms of the variable,  $y=\tilde{R}\Omega=\tilde{P}\Omega$ , and the log-energy scale,  $\Gamma=-\ln \Omega$ , we obtain the differential equations

$$\frac{dy}{d\Gamma} + y^2 = 0, \quad (\text{B7})$$

with the solution

$$y = \tilde{R}\Omega = \tilde{P}\Omega = \frac{1}{\Gamma - \Gamma_0} = \frac{1}{\ln(\Omega_0/\Omega)}, \quad \delta = 0. \quad (\text{B8})$$

Here  $\Gamma_0 = -\ln \Omega_0$  is a reference (log) energy scale. Now, going back to (B3) we can see that at the fixed point the actual value of  $\kappa$  does not matter. The term  $\kappa^{-\Omega \tilde{R}} \rightarrow 1$  and  $\ln \kappa / \ln(\Omega/J) \sim \kappa \tilde{R} \Omega \rightarrow 0$ .

### APPENDIX C: THE RANDOM TRANSVERSE-FIELD ISING MODEL AND ITS DECIMATION RULES

The prototype of random quantum systems is the random transverse-field Ising model which is defined by the Hamiltonian

$$H = - \sum_{\langle i,j \rangle} J_{ij} \sigma_i^x \sigma_j^x - \sum_i h_i \sigma_i^z. \quad (\text{C1})$$

Here the sum runs over nearest neighbors and  $\sigma_i^x$ ,  $\sigma_i^z$  are Pauli matrices at site  $i$ . The exchange couplings  $J_{ij}$  and the transverse-fields  $h_i$  are independently distributed random variables with distributions  $\pi(J)$  and  $\rho(h)$ , respectively. The Hamiltonian in Eq. (C1) in one dimension is closely related to the transfer matrix of a classical two-dimensional layered Ising model, which was first introduced and studied by McCoy and Wu [47].

In the renormalization scheme we have the following decimation relations. If the largest term in the Hamiltonian is a coupling, say  $J=\Omega$ , then the two sites connected by  $J$  and having transverse fields,  $h$  and  $h'$  and moments  $m$  and  $m'$ , behave as an effective composite cluster with moment  $\tilde{m}$  in a renormalized transverse field,  $\tilde{h}$ , which are given by

$$\tilde{h} = \frac{hh'}{J}, \quad \tilde{m} = m + m'. \quad (\text{C2})$$

On the other hand, if the largest term is a transverse field, say  $h=\Omega$ , then the site with this transverse field gives a negligible contribution to the (longitudinal) magnetic susceptibility, thus can be decimated out. This leads to a renormalized coupling between the nearest neighbors of the decimated site that is given by

$$\tilde{J} = \frac{JJ'}{h}, \quad (\text{C3})$$

which is related to (C2) through duality.

- 
- [1] J. Marro and R. Dickman, *Nonequilibrium Phase Transitions in Lattice Models* (Cambridge University Press, Cambridge, 1996).
- [2] R. Dickman, in *Nonequilibrium Statistical Mechanics in One Dimension*, edited by V. Privman (Cambridge University Press, Cambridge, 1997).
- [3] P. Grassberger and A. de la Torre, *Ann. Phys. (N.Y.)* **122**, 373 (1979).
- [4] T. E. Harris, *Ann. Prob.* **2**, 969 (1974).
- [5] R. M. Ziff, E. Gulari, and Y. Barshad, *Phys. Rev. Lett.* **56**, 2553 (1986).
- [6] J. Cardy and U. C. Täuber, *Phys. Rev. Lett.* **77**, 4780 (1996); J. Cardy and U. C. Täuber, *J. Stat. Phys.* **90**, 1 (1998).
- [7] H. Takayasu and A. Y. Tretyakov, *Phys. Rev. Lett.* **68**, 3060 (1992); I. Jensen, *Phys. Rev. E* **47**, 1(R) (1993).
- [8] H. Hinrichsen, *Phys. Rev. E* **55**, 219 (1997).
- [9] J. Kockelkoren and H. Chaté, *Phys. Rev. Lett.* **90**, 125701 (2003).
- [10] M. Rossi, R. Pastor-Satorras, and A. Vespignani, *Phys. Rev. Lett.* **85**, 1803 (2000).
- [11] H. Hinrichsen, *Braz. J. Phys.* **30**, 69 (2000).
- [12] A. L. Barabási and H. E. Stanley, *Fractal Concepts in Surface Growth* (Cambridge University Press, Cambridge, 1995).
- [13] A. Daerr and S. Douady, *Nature (London)* **399**, 241 (1999); H. Hinrichsen *et al.*, *Nature (London)* **83**, 4999 (1999).
- [14] A. J. Noest, *Phys. Rev. Lett.* **57**, 90 (1986).
- [15] A. G. Moreira and R. Dickman, *Phys. Rev. E* **54**, R3090 (1996); R. Dickman and A. G. Moreira, *ibid.* **57**, 1263 (1998).
- [16] H. K. Janssen, *Phys. Rev. E* **55**, 6253 (1997).
- [17] M. Bramson, R. Durrett, and R. H. Schonmann, *Ann. Prob.* **19**, 960 (1991).
- [18] R. Caferio, A. Gabrielli, and M. A. Muñoz, *Phys. Rev. E* **57**, 5060 (1998).
- [19] I. Webman *et al.*, *Philos. Mag. B* **77**, 1401 (1998).
- [20] F. C. Alcaraz *et al.*, *Ann. Phys. (N.Y.)* **230**, 250 (1994).
- [21] G. M. Schütz, in *Phase Transitions and Critical Phenomena*, edited by C. Domb and J. L. Lebowitz (Academic Press, London, 2000), Vol. 19.

- [22] I. Jensen and R. Dickman, *J. Stat. Phys.* **71**, 89 (1993).
- [23] M. Kaulke and I. Peschel, *Eur. Phys. J. B* **5**, 727 (1998); E. Carlon, M. Henkel, and U. Schollwöck, *ibid.* **12**, 99 (1999).
- [24] J. Hooyberghs and C. Vanderzande, *J. Phys. A* **33**, 907 (2000); *Phys. Rev. E* **63**, 041109 (2001).
- [25] S. K. Ma, C. Dasgupta, and C.-K. Hu, *Phys. Rev. Lett.* **43**, 1434 (1979); C. Dasgupta and S. K. Ma, *Phys. Rev. B* **22**, 1305 (1980).
- [26] D. S. Fisher, *Phys. Rev. Lett.* **69**, 534 (1992); *Phys. Rev. B* **51**, 6411 (1995).
- [27] T. Senthil and S. N. Majumdar, *Phys. Rev. Lett.* **76**, 3001 (1996).
- [28] F. Iglói, R. Juhász, and P. Lajkó, *Phys. Rev. Lett.* **86**, 1343 (2001).
- [29] For a review see J. P. Bouchaud and A. Georges, *Phys. Rep.* **195**, 127 (1990).
- [30] D. S. Fisher, P. Le Doussal, and C. Monthus, *Phys. Rev. E* **59**, 4795 (1999).
- [31] J. Hooyberghs, F. Iglói, and C. Vanderzande, *Phys. Rev. Lett.* **90**, 100601 (2003).
- [32] M. Howard, P. Fröjdh, and K. B. Lauritsen, *Phys. Rev. E* **61**, 167 (2000).
- [33] T. M. Liggett, *Stochastic Interacting Systems* (Springer-Verlag, Berlin, 1999).
- [34] F. Iglói and H. Rieger, *Phys. Rev. B* **57**, 11 404 (1998).
- [35] This relation follows from the fact that in a finite system of size,  $l_c$ , the smallest gap in the active phase behaves as  $\epsilon \sim \exp(-\sigma l_c)$ , thus the ground state is degenerate in the thermodynamic limit.
- [36] R. B. Griffiths, *Phys. Rev. Lett.* **23**, 17 (1969).
- [37] Here generally the parameter,  $\kappa$ , should satisfy  $\kappa \geq 1$ , unless the resulting fixed-point distribution is singular, so that the integral with the analytical continuation of  $R(J, \Omega)$ ,  $\int_{\Omega}^{\kappa \Omega} R(J, \Omega) dJ \rightarrow 0$ , for any  $\kappa > 0$ . We shall see that the fixed-point distribution indeed satisfies this condition.
- [38] O. Motrunich, K. Damle, and D. A. Huse, *Phys. Rev. B* **63**, 134424 (2001).
- [39] F. Iglói, *Phys. Rev. B* **65**, 064416 (2002).
- [40] O. Motrunich *et al.*, *Phys. Rev. B* **61**, 1160 (2000).
- [41] D. Karevski *et al.*, *Eur. J. Biochem.* **20**, 267 (2001).
- [42] R. C. Brower, M. A. Furman, and K. Subbarao, *Phys. Rev. D* **15**, 1756 (1977).
- [43] R. Juhász and F. Iglói, *Phys. Rev. E* **66**, 056113 (2002).
- [44] H. Rieger and F. Iglói, *Europhys. Lett.* **45**, 673 (1999).
- [45] J. Hooyberghs, E. Carlon, and C. Vanderzande, *Phys. Rev. E* **64**, 036124 (2001).
- [46] E. Carlon, P. Lajkó, and F. Iglói, *Phys. Rev. Lett.* **87**, 277201 (2001).
- [47] B. M. McCoy and T. T. Wu, *Phys. Rev.* **176**, 631 (1968); **188**, 982 (1969); B. M. McCoy, *ibid.* **188**, 1014 (1969).